The Astrophysical Journal Letters, 717:L37–L41, 2010 July 1 doi:10.1088/2041-8205/717/1/L37

A DEEP *CHANDRA* OBSERVATION OF THE X-SHAPED RADIO GALAXY 4C +00.58: A CANDIDATE FOR MERGER-INDUCED REORIENTATION?

Edmund J. Hodges-Kluck[1], Christopher S. Reynolds[1], M. Coleman Miller[1], and Chi C. Cheung[2,3]
[1] Department of Astronomy, University of Maryland, College Park, MD 20742-2421, USA; ehodges@astro.umd.edu
[2] Space Science Division, Naval Research Laboratory, Washington, DC 20375, USA
Received 2010 April 12; accepted 2010 May 24; published 2010 June 11

ABSTRACT

Although rapid reorientation of a black hole spin axis (lasting less than a few megayears) has been suggested as a mechanism for the formation of wings in X-shaped radio galaxies (XRGs), to date no convincing case of reorientation has been found in any XRG. Alternative wing formation models such as the hydrodynamic backflow models are supported by observed trends indicating that XRGs form preferentially with jets aligned along the major axis of the surrounding medium and wings along the minor axis. In this Letter, we present a deep *Chandra* observation of 4C +00.58, an odd XRG with its jet oriented along the *minor* axis. By using the X-ray data in tandem with available radio and optical data, we estimate relevant timescales with which to evaluate wing formation models. The hydrodynamic models have difficulty explaining the long wings, whereas the presence of X-ray cavities (suggesting jet activity along a prior axis) and a potential stellar shell (indicating a recent merger) favor a merger-induced reorientation model.

Key words: galaxies: active – galaxies: individual (4C +00.58)

1. INTRODUCTION

X-shaped radio galaxies (XRGs) are double-lobed radio galaxies (Leahy & Williams 1984) which also possess a pair of long, faint, centro-symmetric "wings". They have gained notoriety as a possible signature of a rapid (within a few megayears) reorientation of the supermassive black hole (SMBH) spin axis, conceivably induced by galaxy mergers in which either accretion torque or an SMBH merger causes a spin-flip (Rottmann 2001; Merritt & Ekers 2002). In this scenario, wings are "fossils" tracing the prior jet axis which radiatively decay.

However, no convincing case for reorientation has been made in any individual XRG, whereas several lines of evidence support a hydrodynamic origin for the wings. For instance, in most XRGs, the wings are co-aligned with the minor axis of the host galaxy and the jet with the major axis (Capetti et al. 2002; Saripalli & Subrahmanyan 2009). A similar major-axis–radio alignment trend exists in the X-rays (Hodges-Kluck et al. 2010). These results have been interpreted to favor models in which the wings are produced by radio-lobe–gas interaction (Leahy & Williams 1984; Worrall et al. 1995; Capetti et al. 2002). Additionally, no clear signs of mergers have been found in a spectroscopic study of XRG hosts, whereas they may be overpressured (Landt et al. 2010).

In this Letter, we identify 4C +00.58 (Figure 1, classified as a candidate XRG by Cheung 2007) as one of the best candidates for a merger-induced reorientation based on quantities derived from a deep *Chandra X-ray Observatory* observation and publicly available data. Unlike other XRGs, the 4C +00.58 jet is co-aligned with the *minor* axis of its host. Even if only a fraction of XRGs are produced by reorientation, their frequency may be important for estimating *Laser Interferometer Space Antenna* detection rates.

We use a Galactic absorption of $N_{\rm H} = 7.14 \times 10^{20}$ cm^{-2} (Kalberla et al. 2005), as well as the *Wilkinson Microwave Anisotropy Probe* cosmology ($H_0 = 71$ km s^{-1} Mpc^{-1}, $\Omega_\Lambda = 0.73$, and $\Omega_m = 0.27$; Spergel et al. 2007). At a redshift of $z = 0.059$, $1'' = 1.13$ kpc.

2. OBSERVATIONS

We obtained a 93 ks *Chandra* exposure toward 4C +00.58 using the Advanced CCD Imaging Spectrometer[4] (ACIS) and combined it with a 10 ks archival observation (Obs. IDs 10304 and 9274; latter published in Hodges-Kluck et al. 2010). The source is centered at the nominal aim point on the ACIS-S3 chip. The data were reduced with the *Chandra* Interactive Analysis of Observations (CIAO v4.0) software, and spectral fitting was performed with XSPEC (Arnaud 1996). We extracted a 0.3–10 keV bandpass light curve (binned to 600 s) from empty regions to check for background flares, but found no 3σ deviations. The extended emission around 4C +00.58 is less than $45''$ in radius, so we use local background for spectral extraction.

We also use an NRAO[5] Very Large Array (VLA; Thompson et al. 1980) 1.4 GHz map (Hodges-Kluck et al. 2010) and a 4.9 GHz map produced by combining archival snapshot A-array data from Best et al. (1999) and C-array data from program AC406. We use Sloan Digital Sky Survey (SDSS; Adelman-McCarthy et al. 2008) red (623.1 nm) and green (477.0 nm) images from two 54 s exposures of the host (SDSS J160612.68+000027.1) to measure color and magnitude, correcting for the smaller point-spread function of the green images as well as sky background, the 1000-count software bias, and Galactic extinction.

The 1.4 GHz map is shown in the left panel of Figure 1. The primary lobes of the radio galaxy lie nearly on an east–west axis and have a well-defined boundary, whereas the faint wings are oriented in a north–south direction. The jet experiences a dramatic bend (by 60°) just before terminating, and the cocoon in the 1.4 GHz map is notable for a well-defined edge with a

[3] National Research Council Research Associate.

[4] See http://cxc.harvard.edu/proposer/POG/pdf/ACIS.pdf.

[5] The National Radio Astronomy Observatory is a facility of the National Science Foundation operated under cooperative agreement by Associated Universities, Inc.

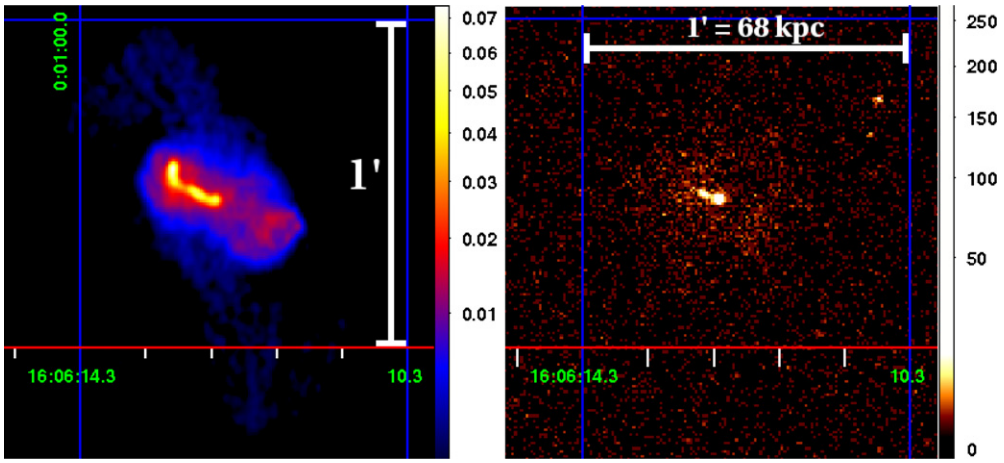

Figure 1. Left: 1.4 GHz VLA A-array map (1.″6 × 1.″3 beam, units in Jy beam^{-1}). Right: raw *Chandra* image (0.3–10 keV). The brightest pixel in the AGN has 282 counts.

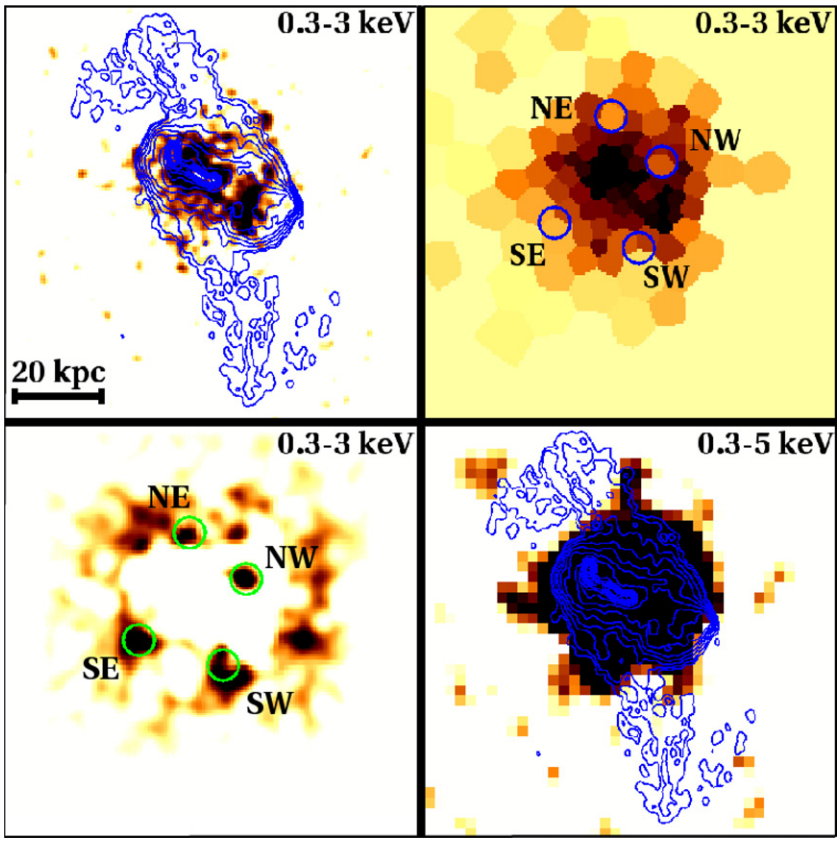

Figure 2. Top left: 1.4 GHz contours overlaid on smoothed ($\sigma = 3$ pixels) X-ray image with point-like sources excised, clipped at twice the mean background. Top right: weighted Voronoi tessellation image (S/N = 5.0 in each tile) of the 0.3–3 keV events with cavities identified. Bottom left: negative of an unsharp mask image of top left (using a smoothing length of 40 pixel for subtraction) showing cavities. Bottom right: coarsely binned (4× native pixels) image from 0.3–5 keV showing extended structures beyond 20 kpc from the AGN.

surface brightness about 5 times that of the wings. The 5 GHz map resolves the jet into a string of knots (Section 3.3). We detect no counterjet.

The X-ray emission (Figure 1) is made up of two components: bright emission spatially associated with the jet/active galactic nucleus (AGN) and a compact diffuse atmosphere. To isolate the atmosphere, we mask point-like sources and restrict the energy bandpass to 0.3–3 keV (Figure 2); this energy range contains 80% of the photons within 45″. On the basis of an unsharp mask image and a weighted Voronoi tessellation adaptively binned image (Diehl & Statler 2006; Cappellari & Copin 2003), we have identified several X-ray cavities (Figure 2). These cavities, labeled C_{NE}, C_{NW}, C_{SE}, and C_{SW}, are low surface brightness regions in the hot atmosphere bounded by "spurs" of greater surface brightness. The cavities are deep negatives in an unsharp mask image in which a heavily smoothed map (40 pixel) is subtracted from a lightly smoothed (3 pixel) map. The residuals are shown in Figure 2.

The SDSS image (Figure 3) reveals a dim, resolved extension to the southwest of the host galaxy. The elliptical host shows

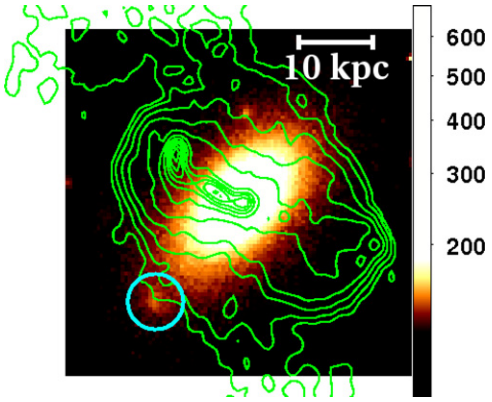

Figure 3. 1.46 GHz contours overlaid on a combined red+green SDSS image of the host galaxy of 4C +00.58. The cyan circle encloses a 20th magnitude resolved "extension" to the elliptical galaxy which is slightly bluer.

no obvious internal structure, but the extension may be a stellar shell from a prior minor merger (for a discussion of shells see Quinn 1984). The extension is red ($g - r \sim 0.7$), but bluer than the host ($g - r \sim 1.0$). The apparent magnitude of the entire extension is $m_r \sim 20$.

3. RESULTS

3.1. Hot Atmosphere

The bright X-ray emission immediately near the jet is nonthermal, otherwise the extended emission is consistent with isothermal plasma out to 50 kpc from the AGN, with $kT = 1.1 \pm 0.2$ keV within 25 kpc and $kT = 0.9 \pm 0.1$ keV outside. The photon statistics preclude a deprojection analysis. On the basis of the resulting emission measures, densities within 25 kpc are a few$\times 10^{-3}$ cm^{-3}, implying pressures $P = 10^{-12}$ to 10^{-11} dyne cm^{-2}. Thus, we adopt a sound speed $c_s \approx 400$ km s^{-1} throughout the region. The total luminosity of the hot atmosphere is $L_X \sim 3 \times 10^{41}$ erg s^{-1}.

The gross morphology of the X-ray emission does not coincide with the host galaxy. Using only the 10 ks exposure, we argued (Hodges-Kluck et al. 2010) that the orientation agreed with the host although the ellipticity did not. With deeper data it is evident that while we correctly excluded nonthermal emission to the southwest, we could not exclude nonthermal emission to the northeast.

The most notable feature of the diffuse X-ray map is C_{NW} (Figure 2), which is collinear with C_{SE} and the AGN. C_{NW} is enclosed by emission and cospatial with a spur in the radio cocoon, suggesting that C_{NW} and C_{SE} are jet-blown cavities. C_{NE} and C_{SW} are also collinear with the AGN and are associated with the bases of the wings, with walls extending into the surrounding medium.

The free–free cooling time of the C_{NW} and C_{SE} bounding material places an upper limit on their ages:

$$t_{\rm ff} \sim \frac{5}{2}\frac{nkT}{\Lambda_{\rm ff}(T)} \approx 1.6 \times 10^9 T_7^{1/2} n_{-3}^{-1}\,{\rm yr} \sim 500\,{\rm Myr}, \quad (1)$$

where $T_7 \sim 1.4$ is the temperature in units of 10^7 K and $n_{-3} \sim 4$ is the density in units of 10^{-3} cm^{-3}. If C_{NW} is a spherical bubble (of radius 5 kpc) inflated at a locally estimated pressure $P = 5 \times 10^{-12}$ dyne cm^{-2}, the work done to inflate it is $W \sim 7 \times 10^{55}$ erg. Since the transonic expansion time is 10 Myr, the minimum average kinetic luminosity of the jet during that period is 2×10^{41} erg s^{-1} if C_{NW} is jet-blown.

3.2. Wings

The long wings are associated with low-signal X-ray structure (Figure 2, bottom right). The approximate wing symmetry implies coherent formation, but the southern wing is slightly longer.

If the wings expanded transonically, their length (∼36 kpc) implies an age of 90 Myr, although this is a minimum age since the wings are seen in projection and may expand subsonically. Conversely, the synchrotron decay time $t_{\rm sync}$ provides a maximum wing lifetime assuming the radio emission traces the entire wing volume and the wings were inflated by the radiating plasma. To estimate $t_{\rm sync}$, we follow Tavecchio et al. (2006) and use the 1.4 GHz map to estimate the equipartition field $B_{\rm eq}$. We take the spectral index, $\alpha = 0.7$ ($S_\nu \propto \nu^{-\alpha}$), from low-resolution radio photometry and assume $\gamma_{\rm min} \sim 10$. For cylindrical wings of $r = 6$ kpc and $h = 36$ kpc, we obtain $B_{\rm eq} \sim 10$ μG. We then find the electron Lorentz factor $\gamma \sim 5600$ from $\nu_{s[1.4{\rm GHz}]} = 4 \times 10^{-3} B\gamma^2 = 1.4$ GHz, and thus find

$$t_{\rm sync} \approx 2.4 \times 10^9 \gamma_4^{-1} B_{\mu\rm G}^{-2}\,{\rm yr} \sim 40\,{\rm Myr}, \quad (2)$$

where γ_4 is in units of 10^4 and $B_{\mu\rm G}$ is in μG. This value represents the cooling time of the 1.4 GHz electrons; we emphasize our assumption that this is "first-generation" plasma occupying the wings. $t_{\rm sync}$ is insensitive to projection effects relative to the transonic expansion time: if the wings are longer by a factor of 2, $B_{\rm eq}$ decreases by a factor $2^{1/(3+\alpha)} \sim 1.2$ and $t_{\rm sync}$ increases by a factor ∼1.4. The disagreement between $t_{\rm sync}$ and the expansion time suggests either supersonic expansion (i.e., like a jet-blown cocoon) or wing replenishment by supersonic inflowing lobe plasma.

The work required to inflate the wings, assuming the cylinders above, is $PdV \sim 10^{57}$ erg. An age of 40 Myr implies an average kinetic luminosity of $L_{\rm kin} \sim 8 \times 10^{41}$ erg s^{-1} applied to the wings alone.

3.3. Nucleus and Jet

The strong central X-ray point source corresponds to the AGN and contains 1100 counts. The spectrum is well fit by a model consisting of an unabsorbed power law with spectral index $\alpha = 0.7 \pm 0.1$ and a weak thermal model frozen at $kT = 1.0$ keV. The nonthermal luminosity is $L_X \sim 7 \times 10^{41}$ erg s^{-1} between 0.3 and 10 keV.

The X-ray jet is the next brightest feature and traces the radio jet well, including several X-ray knots (Figure 4). A super-sampled X-ray image reveals that two of these knots coincide with more compact knots visible in the 5 GHz image and a bright region in the 1.4 GHz jet. There is a modest radio (1.4–5 GHz) spectral gradient between the inner and outer jets (Table 1), and the outer jet does not appear in the X-rays. Along the inner jet, we measure a broadband radio to X-ray spectral index, $\alpha_{rx} \sim 1.0$, which is consistent with the X-ray spectrum ($\alpha_x \sim 1.1 \pm 0.4$). Thus, the X-ray emission is consistent with a synchrotron origin (requiring a concave-down spectral energy distribution). Alternatively, assuming an inverse-Compton origin for the X-rays, we follow Tavecchio et al. (2006) to estimate the jet Doppler factor $\delta = [\gamma(1 - \beta\cos\theta)]^{-1}$ in the knots by finding B such that $B_{\rm eq}\delta = B_{\rm IC}/\delta$. This results in $\delta \sim 10$ (Table 1) and $B_{\rm knot} \sim 10$ μG. As the jet X-ray emission is unlikely dominated by inverse-Compton emission, δ is formally an upper limit. $B_{\rm eq}$ is derived with no knowledge of

Table 1
Core and Jet Parameters

Designation	Distance (″)	$F_{1.4\mathrm{GHz}}$ (mJy)	$F_{4.9\mathrm{GHz}}$ (mJy)	$F_{\mathrm{X-ray}}$ (nJy)	α_r	α_{rx}	α_x	δ	B_{eq} (μG)
Core	0.0	41 ± 4	30 ± 3	$8.3^{+0.7}_{-0.1}$	0.25	0.8	0.7 ± 0.1	···	···
Inner jet	0.6−6.0	180 ± 20	88 ± 9	1.0 ± 0.3	0.6	1.0	1.1 ± 0.4	<7	7
Inner knot 1	2.5	···	14 ± 1	0.3 ± 0.2	0.6[a]	1.0	1.0 ± 0.7	<8	9
Inner knot 2	3.3	···	15 ± 1	0.9 ± 0.3	0.6[a]	0.9	1.5 ± 0.6	<10	7
Outer jet	6.0−10.0	220 ± 20	70 ± 7	<0.1	0.9	>1.1	···	···	$120/\delta$

Notes. Most of the jet X-ray emission comes from knot 2 and the outer jet has no X-ray emission. The distance is measured radially from the core in arcsec. We report a model X-ray flux from the best-fit power-law model with errors reported at 90% confidence.
[a] It is not possible to separate the knots at 1.4 GHz, so we use the average value instead of measuring a flux.

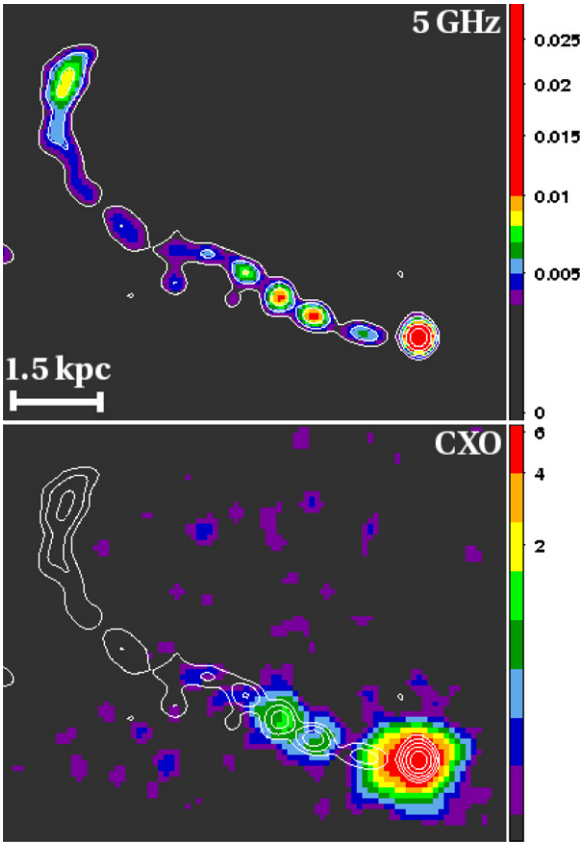

Figure 4. Top: 5 GHz VLA image of the jet with contours (beam size 0.″5 × 0.″5, units in Jy beam^{-1}). Bottom: smoothed X-ray image with pixel randomization turned off (superbinned to 1/4-original pixel size) with 5 GHz contours overlaid.

the X-ray emission and predicts $P \sim 3 \times 10^{-12}$ dyne cm^{-2}, in agreement with spectral fitting estimate.

Although no counterjet is visible, the 1.4 GHz emission suggests the jet has point symmetry. If the jet tail is dragged, the tail will cool radiatively with its length set by the cooling time (i.e., no additional plasma influx). We derive an upper $B_{\mathrm{eq}}\delta \sim 120$ μG at $\nu_s = 5$ GHz and thus find $t_{\mathrm{sync}} \sim 0.5$–15 Myr for $\delta = 1$–10. We assume δ declines along the jet, so for $\delta \sim 5$, $t_{\mathrm{sync}} \sim 6$ Myr.

The projected length of the radio cocoon gives a transonic expansion time of 35 Myr. The work done to excavate a cocoon with semimajor axis $a = 17$ kpc and semiminor axes $b = c = 8$ kpc is $PdV \sim 7 \times 10^{56}$ erg, so the minimum average kinetic luminosity while inflating the cocoon is $L_{\mathrm{kin}} \sim 7 \times 10^{40}$ erg s^{-1}.

4. WING FORMATION MODELS

We consider three wing formation scenarios: an overpressured outburst, conical precession of the jet axis, and merger-induced reorientation of the jet axis.

In the backflow models, wings are produced by pressure- or buoyancy-driven back-flowing plasma from the terminal shocks evolving in the hot medium. Since we see no obvious evidence for a plumed jet *directly* feeding the wings, the most plausible of these models is a "blow-out" from an overpressured cocoon early in the source's life (Capetti et al. 2002). In this model, the native atmosphere confining the young jets is aspherical with a preferential direction along which the cocoon ruptures.

The backflow model suffers from several difficulties. First, the wings must expand at most transonically. The long projected length of the wings in 4C +00.58 (requiring an AGN lifetime of at least 90 Myr) is difficult to reconcile with the cocoon length unless the cocoon inclination angle from the line of sight, θ_{LOS}, is less than 30°. The equivalent widths of O II (3727 Å) and O III (5007 Å) measured by Landt et al. (2010) argue against a steep inclination (Landt et al. 2004). Furthermore, the maximum wing lifetime t_{sync} disagrees with the transonic expansion time, although the wing plasma may be continuously replenished. Second, the model relies on strong backflows typically associated with Fanaroff & Riley (1974, FR) type II sources. 4C +00.58 is not easily classified as FR I or II, but at $M_R \sim -22.7$ and $\log L_r(1.4\ \mathrm{GHz}) \sim 25.3$ W Hz^{-1} falls very close to the Ledlow & Owen (1996) boundary ($L_{\mathrm{radio}} \propto L_{\mathrm{opt}}^{1.8}$). Since XRGs generally lie near the Ledlow & Owen (1996) FR I/II boundary, they may be a transition population (Cheung et al. 2009; Landt et al. 2010). Finally, the radio galaxy is misaligned with its host, so the Capetti et al. (2002) model cannot produce wings until the jet escapes the interstellar medium.

Conical precession is a simple model in which the jet axis swings around, so the wing extensions and post-bend jet are equidistant from the AGN. This requires a steep inclination angle of $\theta_{\mathrm{LOS}} < 30°$. In this model, the wings trace the jet history, and the oldest plasma can be no older than the synchrotron cooling time. To obtain the precession rate $\dot{\phi}$, we compare the projected length of the post-bend jet to its cooling time (about 6 Myr) and obtain $\dot{\phi} \sim 4°$ Myr^{-1} (corresponding to a mildly supersonic $v \sim 460$ km s^{-1}). A 180° rotation takes ~45 Myr and implies supersonic expansion for the cocoon. The timescale is consistent with the wing t_{sync}, but the model must also explain the larger far-side cone, as both the far-side cocoon and wing have longer projected lengths. Notably, precession does not explain the presence of C_{NW} and C_{SE}, and numerical

simulations (e.g., Falceta-Gonçalves et al. 2010) indicate that it would not preserve obvious cocoon structure.

In the reorientation (spin-flip) scenario, the wings are fossil lobes of a jet whose direction rapidly changed, either due to accretion torque or coalescence of an SMBH binary. There is circumstantial evidence for such a spin-flip: a possible stellar shell indicating a minor merger, and the cavities C_{NW} and C_{SE} with overlapping cocoon extensions implying somewhat recent jet–gas interaction along an old axis. We describe a reorientation scenario for 4C +00.58 presently.

Given the small size of C_{NW} and C_{SE}, the jet was in a weak or "off" state prior to the minor merger, but the SMBH spin axis was aligned with the major axis of the host. Upon ignition, the jet quickly formed C_{NW} and C_{SE}. However, since the angular momentum axis of the accreting gas is generally misaligned with that of the SMBH, accretion torque will reorient the black hole's spin within a few megayears (Dotti et al. 2010). Hence, C_{NW} must have expanded at $v_{exp} > 2c_s$ if no prior cavity existed.

Once accretion torque moved the jet to the wing axis, it inflated the wings as active lobes. The transonic lateral expansion time of the wings is 10 Myr, implying $v_{exp} < 8c_s$ during wing inflation. The "Z-shaped" wing extensions (covering 30°) could be explained either as post-reorientation "wiggles" from a hot disk (Dotti et al. 2010, show that a hot disk is required for wiggles of this magnitude) or interaction between the lobes and merging ISM swirling into the host (Gopal-Krishna et al. 2003; Zier 2005). These Z-shaped extensions then evolve buoyantly, and may be replenished by the primary lobes once the jet axis has moved (Gopal-Krishna et al. 2003). We suppose the jet moved to its current position due to coalescence of the SMBH binary or ongoing accretion torque, then formed the present cocoon. Since the jet may have experienced small realignments during the wing inflation phase, we infer a reorientation timescale of fewer than 50 Myr since jet ignition, well within the free–free cooling time of the C_{NW} walls and constrained by the wing t_{sync}. Although it is possible that the system represents only a single spin-flip from the wings to the present location, this hypothesis does not explain C_{NW} or C_{SE}.

The presence of a stellar shell must be confirmed, and it is possible that C_{NW} and C_{SE} are not jet-blown cavities but rather part of a cocoon-evacuated shell (with bounding material describing a ring perpendicular to the jet) produced by a jet-ignition shock wave. The overlap of C_{NW} by the radio cocoon is then due to backflow filling the cavity. Assuming a circular ring, the eccentricity of the ring implies $\theta_{LOS} \sim 60°$, far above the 30° required to reconcile the cocoon and wing lengths.

5. CONTEXT AND SUMMARY

There are few deep X-ray observations of XRGs. Apart from 4C +00.58, there is a ∼100 ks *Chandra* observation of NGC 326 and a 50 ks exposure of 3C 403 (Kraft et al. 2005). These data show X-ray emission on different scales and of differing surface brightness, forcing the hydrodynamic hypothesis to contend with a variety of environments. The cavities in 4C +00.58 also demonstrate that X-ray observations are not only useful for studying backflow models. Our prior survey (Hodges-Kluck et al. 2010) and this study suggest exposure times of at least 100 ks are required to examine detailed structure.

We know of no clean evidence for merger-induced reorientation. Even in our toy model, the wings are produced by merger-induced accretion rather than an instantaneous spin-flip, so the black hole merger itself would involve mostly aligned spins (Bogdanović et al. 2007). Nonetheless, the presence of an apparent stellar shell suggests that searching for structure in the hosts of XRGs may provide strong indirect evidence for such mergers in a subclass of these objects.

We have presented a deep *Chandra* observation of the XRG 4C +00.58. The hot atmosphere is roughly cospatial with the radio galaxy and has a temperature of $kT \approx 1.0 \pm 0.2$ keV. An X-ray jet of about 5 kpc is detected, overlapping well with the 5 GHz knots. We synthesize information from the radio and X-ray maps to assess three wing formation models based on approximate limiting timescales and argue that the hydrodynamic scenario faces several difficulties whereas circumstantial evidence favors the reorientation model. Although 4C +00.58 does not obey the optical–radio correlation of XRGs (Capetti et al. 2002; Saripalli & Subrahmanyan 2009), confirmation of any of the wing formation scenarios would bear on XRG formation generally.

We thank the referee for helpful suggestions and clarification. E.J.H.-K. and C.S.R. thank the support of the *Chandra* Guest Observer program grants GO90111X and GO89109X.

Facilities: CXO, VLA

REFERENCES

Adelman-McCarthy, J., et al. 2008, ApJS, 175, 297
Arnaud, K. A. 1996, in ASP Conf. Ser. 101, Astronomical Data Analysis Software and Systems V, ed. G. H. Jacoby & J. Barnes (San Francisco, CA: ASP), 17
Best, P. N., Röttgering, H. J. A., & Lehnert, M. D. 1999, MNRAS, 310, 223
Bogdanović, T., Reynolds, C. S., & Miller, M. C. 2007, ApJ, 661, L147
Capetti, A., Zamfir, S., Rossi, P., Bodo, G., Zanni, C., & Massaglia, S. 2002, A&A, 394, 39
Cappellari, M., & Copin, Y. 2003, MNRAS, 342, 345
Cheung, C. C. 2007, AJ, 133, 2097
Cheung, C. C., Healey, S. E., Landt, H., Verdoes Kleijn, G., & Jordán, A. 2009, ApJS, 181, 548
Diehl, S., & Statler, T. S. 2006, MNRAS, 368, 497
Dotti, M., Volonteri, M., Perego, A., Colpi, M., Ruszkowski, M., & Haardt, F. 2010, MNRAS, 402, 682
Falceta-Gonçalves, D., Caproni, A., Abraham, Z., Teixeira, D. M., & de Gouveia Dal Pino, E. M. 2010, ApJ, 713, L74
Fanaroff, B. L., & Riley, J. M. 1974, MNRAS, 167, 31P
Gopal-Krishna, Biermann P. L., & Wiita, P. J. 2003, ApJ, 594, L103
Hodges-Kluck, E. J., Reynolds, C. S., Cheung, C. C., & Miller, M. C. 2010, ApJ, 710, 1205
Kalberla, P. M. W., Burton, W. B., Hartmann, D., Arnal, E. M., Bajaja, E., Morras, R., & Pöppel, W. G. L. 2005, A&A, 440, 775
Kraft, R. P., Hardcastle, M. J., Worrall, D. M., & Murray, S. S. 2005, ApJ, 622, 149
Landt, H., Cheung, C. C., & Healey, S. E. 2010, MNRAS, submitted
Landt, H., Padovani, P., Perlman, E. S., & Giommi, P. 2004, MNRAS, 351, 83
Leahy, J. P., & Williams, A. G. 1984, MNRAS, 210, 929
Ledlow, M. J., & Owen, F. N. 1996, AJ, 112, 9
Merritt, D., & Ekers, R. D. 2002, Science, 297, 1310
Quinn, P. J. 1984, ApJ, 279, 596
Rottmann, H. 2001, PhD thesis, Univ. of Bonn
Saripalli, L., & Subrahmanyan, R. 2009, ApJ, 695, 156
Spergel, D. N., et al. 2007, ApJS, 170, 377
Tavecchio, F., Maraschi, L., Sambruna, R. M., Gliozzi, M., Cheung, C. C., Wardle, J. F. C., & Urry, C. M. 2006, ApJ, 641, 732
Thompson, A. R., Clark, B. G., Wade, C. M., & Napier, P. J. 1980, ApJS, 44, 151
Worrall, D. M., Birkinshaw, M., & Cameron, R. A. 1995, ApJ, 449, 93
Zier, C. 2005, MNRAS, 364, 583